Title

Microenvironment influences vascular differentiation of murine cardiovascular progenitor cells

Journal

Journal of Biomedical Materials Research Part B Applied Biomaterials, 102(8)

ISSN

1552-4973

Authors

Gluck, Jessica M
Delman, Connor
Chyu, Jennifer
et al.

Publication Date

2014-11-01

DOI

10.1002/jbm.b.33155

Peer reviewed

Published in final edited form as:

J Biomed Mater Res B Appl Biomater. 2014 November ; 102(8): 1730–1739. doi:10.1002/jbm.b.33155.

Microenvironment influences vascular differentiation of murine cardiovascular progenitor cells

Jessica M. Gluck[1,2], **Connor Delman**[1], **Jennifer Chyu**[2], **W. Robb MacLellan**[2,3], **Richard J. Shemin**[1], **Sepideh Heydarkhan-Hagvall**[1,4]

[1]Department of Surgery, Cardiovascular Tissue Engineering Laboratory, David Geffen School of Medicine, University of California Los Angeles, Los Angeles, California

[2]Department of Medicine, Cardiovascular Research Laboratories, David Geffen School of Medicine, University of California Los Angeles, Los Angeles, California

[3]Division of Cardiology, School of Medicine, University of Washington, Seattle, Washington

[4]AstraZeneca R&D Mölndal, Cardiovascular and Metabolic Diseases iMed, Mölndal, Sweden

Abstract

We examined the effects of the microenvironment on vascular differentiation of murine cardiovascular progenitor cells (CPCs). We isolated CPCs and seeded them in culture exposed to the various extracellular matrix (ECM) proteins in both two-dimensional (2D) and 3D culture systems. To better understand the contribution of the microenvironment to vascular differentiation, we analyzed endothelial and smooth muscle cell differentiation at both day 7 and day 14. We found that laminin and vitronectin enhanced vascular endothelial cell differentiation while fibronectin enhanced vascular smooth muscle cell differentiation. We also observed that the effects of the 3D electrospun scaffolds were delayed and not noticeable until the later time point (day 14), which may be due to the amount of time necessary for the cells to migrate to the interior of the scaffold. The study characterized the contributions of both ECM proteins and the addition of a 3D culture system to continued vascular differentiation. Additionally, we demonstrated the capability bioengineer a CPC-derived vascular graft.

Keywords

cell differentiation; vascular; progenitor cells; stem cells; scaffolds; extracellular matrix

INTRODUCTION

Heart disease is a leading cause of morbidity and mortality in the United States.[1,2] Conventional therapies range from lifestyle changes to drug therapy to surgical intervention, with heart transplantation being the final option.[3,4] Recently, regenerative therapies and stem cell-based approaches in particular have garnered much interest.[5] Stem cells combined with tissue-engineering principles could potentially be used to fabricate cardiovascular tissue,

Correspondence to: S. Heydarkhan-Hagvall (Sepideh.Hagvall@astrazeneca.com).

which can be used as both a more realistic *in vitro* culture model and potentially as tissue replacement for heart disease patients *in vivo*. One such example is stem cell niches. Much work has been conducted to determine what comprises the niche environment of cardiac progenitor cells (CPCs) found in small populations *in vivo* and the mechanisms by which this cell population then differentiates to form committed cardiovascular tissue.

In vivo, endogenous stem cells reside in tissue-specific anatomically defined clusters called "niches." The idea of the stem cell niche was first proposed by Schofield almost 35 years ago as he studied mammalian haematology.[6] Within the stem cell niche, cell fate is thought to be controlled both spatially and temporally, as well as through cell–cell and cell–matrix interactions. Paracrine and autocrine effects are also thought to regulate cell fate within the niche—there is mounting evidence that stem cells secrete a variety of growth factors, cytokines, chemokines, and bioactive lipids which regulate biology and interactions within the surrounding microenvironment. These factors are thought to inhibit apoptosis, stimulate proliferation, and promote vascularization.[7] Additionally, interactions with resident niche cells or the surrounding niche extracellular matrix (ECM) are thought to play an equally important role.

CPCs are thought to reside in niches found in the developing right atria, ventricle, and outflow tract. A small endogenous population of CPCs in the adult myocardium exists which are able to repair small damages.[8] Stem cells are able to initially differentiate to this CPC state.[9,10] These progenitor cells are at one of the earliest stages in mesodermal differentiation toward a cardiovascular lineage. Because the ECM contributes to cell-fate decisions, it makes the native CPC niche ECM's role in vascular development very important to understand. In the absence of signals coming from the ECM, cells can undergo apoptosis. Various studies have shown the importance of ECM support necessary for angiogenesis and vascular physiology.[11] However, the exact nature of the ECM's role during vascular development is still unknown.

Vascular tissue engineering presents an opportunity to not only attempt recreate native tissue *in vitro* but also gain a better understanding of how the tissue develops.[2,3,12] Tissue-engineered structures could also be used to create bioengineered vascular grafts to reinforce a weakened tissue and promote endogenous healing properties, as well as potentially replace damaged/diseased tissues[13–15] in a more sustainable manner than current synthetic grafts. Development of three-dimensional (3D) scaffolds that mimic the natural fibrous ECM can allow for diffusion of nutrients, metabolites, and soluble factors necessary to the seeded cells until they are able to produce their own functional ECM.[15,16] Electrospinning technology can be utilized to create customized electrospun nonwoven mats consisting of essentially any polymer and create microenvironments on which different cell types have been known to proliferate and thrive.[16–21]

More specific to the CPC niche environment, we have shown that CPC commitment and further differentiation can be directed by the microenvironment and that an *in vitro* 3D culture model can be used to promote cardiovascular differentiation in a mouse embryonic stem (ES) cell model by adding both ECM proteins and a 3D electrospun scaffold.[22] Further

studies demonstrated that laminin- or vitronectin-coated 3D scaffolds induced an even higher population of Flk-1$^+$ CPCs as compared to 2D culture conditions.[23]

We aim to determine the role of the microenvironment on further committed vascular differentiation of mouse CPCs using electrospun scaffolds and ECM proteins to create an *in vitro* 3D culture system. By understanding the contribution of the microenvironment to vascular differentiation, we can use that knowledge to direct differentiation to ultimately create a CPC-derived vascular graft.

MATERIALS AND METHODS

Mouse ES cell culture

Murine ES v6.5 cells were purchased from Open Biosystems. mES cells were maintained in an undifferentiated, feeder-free state in leukemia inhibitory factor (LIF) supplemented medium (Knockout Dulbecco's modified Eagle's medium, Invitrogen, Carlsbad, CA) with 15% ES-FBS (Invitrogen), 0.1 m*M* β-mercaptoethanol, 2 m*M* L-glutamine (Invitrogen), 0.1 m*M* nonessential amino acids (Invitrogen), 1000 U/mL recombinant LIF (Chemicon, Temecula CA), and 2 m*M* HEPES (Invitrogen). Cells were cultured on gelatin-coated (0.1% gelatin in PBS, coated for 2h at 37°C) T-75 flasks at 37C, 5% CO_2 in a humidified incubator. Cells were passaged every 2–3 days to maintain an undifferentiated state.

For initial differentiation assays, mES cells were introduced to collagen IV flasks (BD Biosciences, San Jose, CA) and maintained in α-minimum essential medium (α-MEM) (Invitrogen) supplemented with 10% ES-FBS (Invitrogen), 0.1 m*M* β-mercaptoethanol, 2 m*M* L-glutamine (Invitrogen), 0.1 m*M* nonessential amino acids (Invitrogen), and 2 m*M* HEPES (Invitrogen). Media was refreshed daily. After 5 days, cells were isolated for magnetic-activated cell sorting (MACS).

MACS and differentiation assays

To induce differentiation into Flk-1$^+$ cardiovascular progenitors, undifferentiated mES cells were detached from the collagen IV flasks using TrypLE Select (Invitrogen) after 5 days as described previously.[22,23] To purify a Flk-1$^+$ population, indirect MACS (Miltenyi Biotec, Auburn CA) was used. Cells were pelleted via centrifugation and resuspended in MACS rinsing buffer supplemented with 2% ES-FBS and incubated with rat anti-mouse Flk1 antibody (1:200, BD Pharmingen, San Diego, CA) at 4°C for 20 min. Cells were then washed, pelleted, and resuspended in rinsing buffer with magnetic microbeads (20 μL beads + 80 μL buffer per 10^6 cells, Miltenyi Biotec) and incubated at 4°C for 15 min. Cells were again washed, pelleted, and resuspended in 500 μL rinsing buffer. The cell suspension was run through an MS-column and MiniMACS separator to purify the Flk-1$^+$ population per manufacturer's instructions. Cells were, then, used for differentiation experiments.

For differentiation assays, the mES cells were either cultured on 2D plates coated with collagen IV (ColIV, 5 μg/cm^2, BD Biosciences, San Jose, CA), laminin (5 μg/cm^2, BD Biosciences), fibronectin (5 μg/cm^2, Sigma), vitronectin (50 nm/cm^2, Chemicon), and gelatin (0.1% w/v in sterile PBS) or 3D electrospun scaffolds coated with collagen IV, laminin, fibronectin, vitronectin, and gelatin following the same protocol as 2D dishes. The

ECM coatings of both 2D and 3D surfaces were evaluated by fluorescence for the presence of the protein every 2–3 days for the duration of the longest time point (day14). All proteins were present at comparable levels at each evaluation (data not shown). Cells were maintained in smooth muscle growth medium (SmGM-2; Lonza, Walkersville, MD) supplemented with 10 ng/mL platelet-derived growth factor-BB (PDGF, R&D Systems Inc, Minneapolis, MN) for SMC differentiation or endothelial growth medium (EGM-2; Lonza) supplemented with 50 ng/mL vascular endothelial growth factor (VEGF, R&D Systems) for EC differentiation for up to 14 days at 37°C and 5% CO^2.

Electrospun scaffold fabrication

Electrospinning has been used to produce scaffolds with nanodiatmeter to microdiameter fibers with a similar 3D nature to the ECM as described before.[24] Briefly, gelatin type B (bovine skin 10% w/v, Sigma-Aldrich) and ϵ-polycaprolactone (PCL, 10% w/v, Sigma-Aldrich) were mixed together and dissolved in 1,1,1,3,3,3-hexafluoro-2-propanol (HFP, Sigma-Aldrich) to form the outer sheath solution. A core solution of polyurethane (PU, 5% w/v, Sigma-Aldrich) was dissolved in HFP. The positive output lead of a high voltage supply (28 kV; Glassman High Voltage, NJ) was attached to the syringe system and a flow rate of 70 μL/min was used. A dry fibrous scaffold was collected in the form of a 3D mat (100–200-μm thick). The electrospun scaffolds were, then, sterilized by soaking the scaffolds in 70% ethanol for 30 min at room temperature. After three washes of sterile PBS, the scaffolds were aseptically cut into 1 × 1 cm squares and statically coated with colIV, fibronectin, laminin, and vitronectin as described previously in MACS and differentiation assays section. Cells were, then, seeded statically on top of the scaffolds.

Tubular structures were fabricated by collecting randomly aligned nanofibers on a grounded rotating mandrel in lieu of a flat copper collection plate, as seen in Figure 1(A). The tubular structures were approximately 2 cm in diameter and 300–500 μm in thickness, having an inner diameter of about 1.5–1.8 cm [Figure 1(A), bottom panel]. They were sterilized with 70% ethanol and placed in a bioreactor system, LumeGen V60 (Tissue Growth Technologies, Minnetonka, MN). A pump source (Masterflex L/S pump head and drive, Cole-Parmer, Vernon Hills, IL) was used to introduce a flow of media through the lumen of the electrospun tubular scaffold at a constant pressure of 120 mmHg [as seen in Figure 1(B)]. Flk-1^+ CPCs were isolated as described and 5×10^6 were seeded in a small volume (approximately 100 μL cell suspension) in the lumen (inner diameter) of the tubular scaffold; the inner diameter is clearly shown in the bottom panel of Figure 1(A). Cells were maintained in smooth muscle cell growth media. The exterior of the scaffold was also maintained in smooth muscle cell growth media. The entire bioreactor system was rotated 90° approximately every 12 h for the first 3–4 days, and then, the media flow was applied for about 2 week. A second cell seeding of 5×10^6 Flk-1^+ CPCs was, then, seeded in the lumen of the same scaffold and maintained in endothelial cell growth media. The media reservoir was also changed to endothelial cell growth media to supply the media flow in the lumen of the scaffold. The exterior of the scaffold remained maintained with smooth muscle cell growth media.

Immunofluorescence

The mES cells plated on ECM-coated culture slides as well as undifferentiated mES cells were washed and fixed with 4% paraformaldehyde, for 20 min and rinsed with PBS. Slides were, then, blocked with 1% bovine serum albumin (BSA) and 2% goat serum in PBS for 1 h at room temperature. Slides were, then, incubated with primary antibodies (smooth muscle-specific markers: SM-α-actin (Dako, Carpinteria, CA) and SM-myosin (Sigma); endothelial-specific markers: VE-cadherin (CD144, Santa Cruz Biotechnology, Santa Cruz, CA), and von Willebrand Factor (vWF, Dako)) for 1 h at room temperature or overnight at 4°C followed by several washes with PBS. Alexa Fluor 488- or 546-conjugated secondary antibodies (Molecular Probes, Eugene, OR) were applied to the samples and incubated for 30 min at room temperature. After several washes, the cells were counterstained with 4′−6-diamidino-2-phenylindole followed by mounting ProLong Gold antifade mounting medium (Molecular Probes, Carlsbad, CA). Staining without primary antibodies served as controls. Digital images were acquired using a Leica DM IRB inverted microscope system equipped with 20× (0.40 numerical aperture [NA]) and 40× (0.75 NA) objectives (Leica Microsystems, Bannockburn, IL).

Fluorescence-activated cell sorter (FACS) analysis

Cells were harvested from both 2D (conventional culture) and 3D (scaffold) culture, pelleted via centrifugation, washed in FACS buffer (sterile PBS supplemented with 1% ES-FBS, 2% BSA, and 0.25% saponin), and stained with primary antibodies (smooth muscle marker: SM-myosin; endothelial cell marker: CD31). The cells were gated by forward scatter versus side scatter to eliminate debris. A minimum of 10,000 events was counted for each analysis. All analyses were performed using a Becton Dickinson FACS can analytic flow cytometer (BD Biosciences) with FCS Express software (DeNovo Software, Thornhill, ON, Canada) at the UCLA Flow Cytometery Laboratory.

Bioreactor analysis

For ultrastructural analysis, unseeded tubular scaffold samples were processed for characterization by scanning electron microscopy (SEM) as described previously.[24] Fiber samples were cut from different, randomly selected locations on the tubular scaffold to obtain representative fibers from both the inner and outer circumferences. The samples were mounted onto stubs and sputter coated with gold/palladium (Au/Pd to a thickness of ~10 μm) using Denton Desk II before scanning with a JEOL 6610 Low-Vacuum SEM (JEOL, Tokyo, Japan). Fiber diameters in the electrospun scaffolds were measured on scanning electron micrographs. Average fiber diameter was determined from measurements taken perpendicular to the long axis of the fibers within representative microscopic fields (50 measurements per field). The pores formed at the interstices of the fibers were measured using ImageJ software (free download available at http://rsbweb.nih.gov/ij/). For each sample, at least five scanning electron micrographs at 2000× magnification were used for image analysis and pore-size measurement.

After 30 days, the electrospun tubular scaffolds were removed from the bioreactor chamber and fixed in 4% PFA. The tubular scaffolds were cut perpendicular to the lumen as well as parallel to obtain a representative sample of both the cross-section of the cell-seeded tubular

scaffold and the inner and outer cell layers. Samples were, then, paraffin-embedded and prepared for immunofluorescence staining as previously described in Immunofluorescence section.

Statistical analyses

All results are presented as mean values ± standard error of mean (SEM). Statistical significance was assessed by a general linear model, which was fit with main effects for time points (day 7 or day 14), environment (2D or 3D), and protein (ECM proteins of interest: gelatin, collagen IV, laminin, fibronectin, or vitronectin), and two-way interaction terms (environment x protein, environment x day, and day x protein). The interaction terms were left in the model even if they were not statistically significant as these terms helped to explain some of the total variability and consumed a relatively small number of degrees of freedom. $p < 0.05$ were defined as statistically significant.

RESULTS

As depicted in Figure 2, we first expanded mES v6.5 cells, then, exposed them to initial differentiation conditions in α-MEM media. After 5 days, we isolated Flk-1^+ CPCs using the MACS system, and then, seeded the CPCs in both 2D and 3D microenvironments for either 7 or 14 days in both vascular endothelial and smooth muscle cell-specific culture media. Flk-1 or VEGF receptor 2 (VEGF-R2) was used as our CPC marker as previously shown as a reliable CPC marker.[22]

Immunofluorescence imaging

We were able to successfully differentiate the isolated CPCs into all the main vascular lineages—vascular endothelial cells (Figure 3) and vascular smooth muscle cells (Figure 4) as shown by immunofluorescence. Examining the endothelial cells in Figure 3, we see that all four ECM proteins of interest (collagen IV, laminin, fibronectin, and vitronectin) are able to support vascular endothelial cell differentiation. It appears that laminin [Figure 3(B,F)] and vitronectin [Figure 3(D,H)] cultures exhibit a slightly delayed differentiation pattern, as the signal for vWF, a marker of more mature endothelial cells, is faint at both day 7 and day 14. Collagen IV cultures exhibit VE-cadherin at both time points [Figure 3(A,E)], while fibronectin appears to support the most robust differentiation, as evidenced by the strong positive signal of vWF at day 14 [Figure 3(G)]. Figure 4 examines the smooth muscle cell differentiation of the CPCs. All four ECM proteins supported smooth muscle cell differentiation with no discernible difference between the two time points evaluated (Figure 4). Further physiological phenotyping including matrigel vessel assay, as well as carbachol-induced contraction was conducted previously.[23] Thus, isolated CPCs differentiate to vascular endothelial and smooth muscle cells.

FACS

We analyzed the percentage of endothelial and smooth muscle cells via FACS analysis at day 7 and day 14. Figure 5 shows the expression of CD31 (also known as Pecam), a well-known vascular endothelial marker in both 2D and 3D culture. At day 7, the only cultures that exhibit a higher expression of CD31 in 3D are gelatin (2D 25.34 ± 8.08% 3D 34.61 ±

0.49%) laminin (2D 52.61 ± 9.04% 3D 60.38 ± 3.57%). A significant increase was observed in percentage of cells expressing CD31 at day 14 compared to day 7 ($p < 0.05$), as well as a significant difference among the ECM proteins evaluated ($p < 0.0001$) using pairwise statistical comparison. We observed increased differentiation on 3D cultures at the later time point (day 14) for gelatin (d7: 3D 34.61 ± 0.49%, d14: 3D 77.62 ± 1.51%), collagen IV (d7: 3D 31.36 ± 12.76%, d14: 3D 47.83 ± 23.15%), and fibronectin (d7: 3D 17.62 ± 3.48%, d14: 3D 60.17 ± 9.26%). We also observed an increased differentiation on laminin in 2D at the later time point (d7: 2D 52.61 ± 9.04%, d14: 2D 95.81 ± 0.37%). Although we did observe an increase in CD31 expression for collagen IV in 3D culture at the later time point, there was no significant change in 2D culture. Vitronectin in 3D culture experienced a significant decrease in CD31 expression at day 14 (d7: 3D 51.02 ± 7.98%, d14: 3D 30.03 ± 1.19%) while the expression in 2D cultures remained relatively constant. Overall, we observed little difference in CD31 expression between the time points for 2D cultures (except for laminin). We did observe an increase in differentiation at the later time points for three of the ECM proteins (gelatin, collagen IV, and fibronectin).

We evaluated smooth muscle cell differentiation via FACS analysis using smooth muscle-myosin as a marker as seen in Figure 6. Unlike the endothelial cells, we observed a clear trend of increased myosin expression in 3D cultures at the later time points. We see significantly higher SM-myosin expression in 3D cultures as compared to 2D cultures ($p < 0.0001$), as well as a significant difference between the mean effect of day 7 compared to day 14 ($p < 0.0001$) and all the ECM proteins evaluated ($p < 0.0001$). Both 2D and 3D cultures for gelatin exhibited comparable SM-myosin expression at day 7, (d7: 2D 38.38 ± 0.36% 3D 27.78 ± 1.44%) and there was a significant increase in expression for 3D culture at day 14 (d14: 2D 9.22 ± 0.3%, 3D 36.04 ± 4.24%) but a decrease for expression in 2D culture. Collagen IV and laminin also demonstrated a similar pattern—an increase in expression in 3D at the later time point, but a decrease in 2D culture (Collagen IV d7: 2D 20.53 ± 0.88%, 3D 11.89 ± 1.102%; d14: 2D 7.93 ± 0.10%, 3D 23.04 ± 0.80%; Laminin d7: 2D 17.33 ± 1.69%, 3D 36.52 ± 0.65%; d14: 2D 8.13 ± 0.15%, 3D 32.75 ± 0.64%). Fibronectin exhibited a significantly higher expression of SM-myosin of all cultures at day 7 (d7: 2D 73.57 ± 2.20%, 3D 82.57 ± 0.56%) while there was still a higher level of expression for 3D cultures compared to 2D cultures at day 14 it was a lower level expression compared to the earlier time point (d14: 2D 46.69 ± 1.34%, 3D 70.79 ± 2.27%). Vitronectin remained relatively constant for both time points, with expression of SM-myosin remaining higher for 3D cultures than 2D cultures (d7: 2D 28.63 ± 7.67%, 3D 39.89 ± 6.66%, d14: 2D 18.71 ± 0.35%, 44.69 ± 1.18%). Overall, we see a trend of progressive differentiation over time for 3D cultures compared to 2D cultures and the robust differentiation for fibronectin cultures.

Bioreactor analysis

By creating a tubular scaffold, we aimed to seed the interior lumen of the scaffold with Flk-1^+ CPCs and maintain them using our bioreactor system. The goal was for the cells to migrate into the scaffold while maintaining a constant pressure and pulsatile flow mimicking physiologically relevant systems. After a time period of 14 days, we introduced freshly isolated CPCs to the lumen of the scaffold to create a layered tissue-engineered structure. The newly differentiating CPC-derived vascular smooth muscle cells should have migrated

to the outer most layer of the tubular scaffold while the new CPCs would remain on the inner most layer of the lumen of the scaffold. These CPCs were exposed to endothelial differentiation conditions. Using the information determined from the initial studies, prior to seeding the first CPCs we coated the interior lumen of the scaffold with fibronectin (as described in MACS and differentiation assays section) to promote vascular smooth muscle cell differentiation.

We analyzed the physical properties of the electrospun tubular scaffold in Figure 7. We observed a significant difference in the fiber size and fiber diameter of the fibers found on the lumen [Figure 7(D–F)] of the tubular scaffold compared to the outer circumference [Figure 7(A–C)]. We found significantly smaller fibers on the outer most layer, with an average fiber size of 0.47 + 0.05 μm and an average pore size of 1.78 + 0.25 μm^2 [Figure 7(A–C)]. The fibers in the lumen were larger with an average fiber size of 6.38 + 0.92 μm and an average pore size of 55.36 + 11.07 μm^2 [Figure 7(D–F)].

Immunofluorescence staining was performed on the sections of the Flk-1^+ CPC seeded electrospun tubular scaffolds. A cross-section of the tubular scaffold shows cells distributed throughout the tubular scaffold after 30 days of culture and flow through the lumen of the scaffold in the bioreactor chamber [Figure 8(A), lumen is denoted as “L” with lines indicating the borders of the scaffold]. We, then, analyzed the scaffolds for evidence of the endothelial and smooth muscle cell layers. By seeding the CPCs at staggered time points under cell-specific culture media conditions, we aimed to create a layer of smooth muscle cells on the outer most circumference of the scaffold by maintaining the first CPCs seeded in smooth muscle cell growth media. The second set of CPCs was maintained in endothelial cell growth media in efforts to create an endothelial layer on the inner lumen of the tubular scaffold. The second CPCs seeded were labeled with GFP for the first experiment to establish the existence of cell layers. Further studies did not use GFP-labeled cells so they could be immunostained without GFP interference. We can see in Figure 8(B) that there is a higher number of green fluorescence found in the inner lumen of the tubular scaffold (amount of GFP^+ cells is shown with *). It is a subtle observation as the fibers of the scaffold absorb any fluorochrome or dye, but the GFP-labeled CPCs are found in the lower right corner of panel 8B, which confirms the existence of cell layers. There is evidence of GFP^+ cells throughout the tubular scaffold; however, the greatest amount is found on the inner most area (lumen). We also performed cell type specific immunofluorescence staining for endothelial cells (CD31) and smooth muscle cells (SM-myosin). Again, there is a subtle distinction between the presence of marker-positive cells compared to the fibers. However, we are able to see a higher fluorescence for $CD31^+$ cells on the lumen (inner most circumference of the tubular scaffold, labeled “I” and concentration of $CD31^+$ cells is shown with *) in Figure 8(C). In Figure 8(D), we are able to detect the subtle distinction of a concentration area of SM-$myosin^+$ cells on the outer most circumference of the tubular scaffold (labeled “O” and concentration of SM-$myosin^+$ cells is shown with *). This is further evidence of the creation of CPC-derived layers.

DISCUSSION

A major barrier to developing new treatment strategies for cardiovascular disease is the lack of understanding of the development of the native tissue. To elucidate the complicated role of the stem cell niche in cell-fate decisions, we used a 3D culture system in conjunction with known vascular ECM proteins. Matrigel has been used previously as a 3D substrate, but is ill defined and inconsistent in composition, making it difficult to determine the exact microenvironment contributions.[25] In this study, we attempted to recapitulate the niche microenvironment to understand the role it plays in more committed vascular differentiation.

We have determined that native ECM proteins contribute to the induction of a CPC population previously.[22,23] We, then, wanted to determine the effects of the microenvironment on continued differentiation. By creating nanofibrous scaffolds and coating them with various ECM proteins, we are able to isolate individual protein contributions as well as determine the impact of a 3D environment on committed differentiation. We focused on the differentiation of endothelial and smooth muscle cells to ultimately better understand vascular differentiation.

Native vessels consist of a layer of endothelial cells on the lumen side of the vessel and several layers of smooth muscle cells on tunica adventitia.[26] The endothelial layer is meant to prevent thrombosis, filter fluid, maintain blood vessel tone, and hemostasis and have a role in hormone trafficking, while the smooth muscle layer is to provide mechanical integrity and contraction. Previous studies have shown the ability to create artificial blood vessels or tissue-engineered vascular grafts with limited capabilities. Heparin has been used to promote endothelial cell proliferation but failed to support smooth muscle cell growth.[27] PCL has been used to create scaffolds to use for vascular tissue engineering, with success when immobilized VEGF has also been incorporated.[28]

Our PCL scaffolds have previously been shown to withstand prolonged cell culture but require additional mechanical integrity for use in tissue-engineering applications.[24] We have demonstrated that the microenvironment does have an effect on continued committed differentiation. We observed that laminin and vitronectin enhance endothelial cell growth. Laminin has been shown to exist in myocardium, while vitronectin has been found in native blood vessels.[29] Both of these proteins were used in composite scaffolds, which have been used successfully as cardiac repair platforms.[29] Additionally, laminin has been shown to assist in endothelial cell growth in the retina.[30] Vitronectin was previously shown to enhance CPC populations.[23] Fibronectin was observed to enhance vascular smooth muscle cell growth. This was expected as fibronectin has a close, well-documented relationship with VEGF and vasculogenesis.[31–33] Scaffolds consisting of a fibronectin component have been shown to enhance endothelialization and vascular differentiation for vascular grafts or artificial vessels.[34–37] We were surprised to see that fibronectin did not have as great of an effect on endothelial cell differentiation as it did on the vascular smooth muscle cells.

The addition of a 3D microenvironment did not seem to greatly enhance endothelial cell differentiation. An overall trend of differentiation was not obvious from our limited analysis. We suspect this is due to the nature of endothelialization and the process of vasculogenesis

creating its own 3D structure. Perhaps our scaffold was too constricting to the natural process of vasculogenesis. This is an area of study we wish to pursue further. There was a significant improvement differentiation into vascular smooth muscle cells that were cultured on the 3D scaffolds. We observed the improvement at the later time point (day 14), which is due to the amount of time required for cells to migrate to the interior of the scaffold as determined previously.[24]

Through our studies for optimizing vascular differentiation, we were able to create a layered vascular graft using a bioreactor system. Small diameter vascular grafts with longterm functionality have been extremely hard to create. Synthetic grafts for large vessels have shown great success, however, the “gold standard” for replacement for a small vessel is to use an autologous graft.[38] Synthetic small diameter vascular grafts have problems with the lack of endothelialization on the luminal surface, which can lead to intimal hyperplasia formation and thrombosis.[39–41] Previous studies have focused on improving endothelialization through the addition of fibronectin and other factors, including the Flameng group[35] which created knitted polyester grafts that were coated with fibronectin and a stem cell homing factor SDF-1α. These grafts had marked success with improved endothelialization in a sheep model. Mun et al.[42] created electrospun scaffolds to use for small diameter vascular grafts. The group was able to electrospin a PCL-PLA copolymer to use *in vitro* with successful results. Zhao et al.[43] created cellular sheets from mesenchymal stem cells, which they then fabricated into a tubular structure and implanted in a rabbit model. These constructs showed complete endothelialization after 4 weeks. This study is one of the few that combines synthetic scaffolds with ES cell-derived progenitors to create a layered structure. We have only demonstrated the proof of concept for this system—that we are able to create an ES cell-derived layered vascular graft, which is a novel development. This relatively simple system can be used in the future to recreate physiologically relevant situations, such as hypertension or chronic overload to examine the cellular effects to further understand the origins of disease as well as potentially being used as a new treatment option vascular disease.

CONCLUSIONS

We have characterized the effects of the microenvironment on differentiation of CPCs. After determining that the addition of a 3D microenvironment greatly enhances the induction of a CPC population, we aimed to determine if those effects were translated to later stages of differentiation as the CPCs continued to differentiate down a vascular pathway. We found that laminin and vitronectin enhanced vascular endothelial cell growth in a traditional 2D cell culture system, while fibronectin enhanced vascular smooth muscle cell growth in a 3D system. The 3D system exhibited greater effects on differentiation at later time points, which is due to the longer amount of time necessary for cells to migrate to the interior of the scaffold. We have also created a layered tissue-engineered vascular graft using our 3D scaffolds and time dependent cell-seeding protocol. Overall, we have enhanced our understanding the contributions of the microenvironment to vascular differentiation and how to apply that knowledge to develop new treatment strategies.

ACKNOWLEDGMENT

The authors thank Dr. Chuck Wakeford for his assistance with our statistical analysis.

Contract grant sponsor: Ruth Kirschstein National Research Service Award(J.M.G.); contract grant number: T32HL69766

Contract grant sponsor: Tyler Gilbert Heart Transplant Survivor's Foundation in Heart Research

Contract grant sponsor: Department of Surgery at UCLA

REFERENCES

1. Malik S, Wong ND, Franklin SS, Kamath TV, L'Italien GJ, Pio JR, Williams GR. Impact of the metabolic syndrome on mortality from coronary heart disease, cardiovascular disease, and all causes in United States adults. Circulation 2004;110:1245–1250. [PubMed: 15326067]
2. Hunt SA, Baker DW, Chin MH, Cinquegrani MP, Feldman AM, Francis GS, Ganiats TG, Goldstein S, Gregoratos G, Jessup ML, Noble RJ, Packer M, Silver MA, Stevenson LW, Gibbons RJ, Antman EM, Alpert JS, Faxon DP, Fuster V, Jacobs AK, Hiratzka LF, Russel RO, Smith SC. ACC/AHA Guidelines for the evaluation and management of chronic heart failure in the adult: Executive Summary; A report of the American College of Cardiology/American Heart Association Task Force on practice guidelines (committee to revise the 1995 guidelines for the evaluation and management of heart failure): Developed in collaboration with the International Society for Heart and Lung Transplantation, Endorsed by the Heart Failure Society of America. Circulation 2001;104:2996–3007. [PubMed: 11739319]
3. Ornish D, Brown SE, Scherwitz LW, Armstrong WT, Ports TA, McLanahan SM, Kirkeeide RL, Gould KL, Brand RJ. Can lifestyle changes reverse coronary heart disease? Lancet 1990;336:129–133. [PubMed: 1973470]
4. Fonarow GC, Gawlinski A, Moughrabi S, Tillisch JH. Improved treatment of coronary heart disease by implementation of a cardiac hospitalization atherosclerosis management program (CHAMP). Am J Cardiol 2001;87:819–822. [PubMed: 11274933]
5. Heydarkhan-Hagvall S, Schenke-Layland K, Dhanasopon AP, Rofail R, Smith H, Wu BM, Shemin R, Beygui RE, MacLellan WR. Three-dimensional electrospun ECM-based hybrid scaffolds for cardiovascular tissue engineering. Biomaterials 2008;29:2907–2914. [PubMed: 18403012]
6. Schofield R The relationship between the spleen colony-forming cell and the haemopoietic stem cell. Blood Cell 1978;4:7–25.
7. Ratajczak MZ, Kucia M, Jadczyk T, Greco NJ, Wojakowski W, Tendera M, Ratajczak. Pivotal role of paracrine effects in stem cell therapies in regenerative medicine: Can we translate stem cell-secreted paracrine factors and microvesicles into better therapeutic strategies? Leukemia 2012;26:1166–1173. [PubMed: 22182853]
8. Mouquet F, Pfister O, Jain M, Oikonomopouls A, Ngoy S, Summer R, Fine A, Liao R. Restoration of cardiac progenitor cells after myocardial infarction by self-proliferation and selective homing of bone marrow-derived stem cells. Cir Res 2005;97:1090–1092.
9. Heydarkhan-Hagvall S, Schenke-Layland K, Yang JQ, Heydarkhan S, Xu Y, Zuk PA, MacLellan WR, Beygui RE. Human adipose stem cells: A potential source for cardiovascular tissue engineering. Cells Tissues Organs 2008;187:263–274. [PubMed: 18196894]
10. Schenke-Layland K, Rhodes KE, Angelis E, Butylkova Y, Heydarkhan-Hagvall S, Gekas C, Zhang R, Goldhaber JI, Mikkola HK, Plath K, MacLellan WR. Reprogrammed mouse fibroblast differentiate into cells of the cardiovascular and hematopoietic lineages. Stem Cells 2008;26:1537–1546. [PubMed: 18450826]
11. Ingber DE. Mechanical signaling and the cellular response to extracellular matrix in angiogenesis and cardiovascular physiology. Circ Res 2002;91:877–887. [PubMed: 12433832]
12. Malik S, Wong ND, Franklin SS, Kamath TV, L'Italien GJ, Pio JR, Williams GR. Impact of the metabolic syndrome on mortality from coronary heart disease, cardiovascular disease, and all causes in United States adults. Circulation 2004;110:1245–1250. [PubMed: 15326067]

13. Nerem RM. Tissue engineering: Confronting the transplantation crisis. Proc Inst Mech Eng [H] 2000;214:95–99.
14. Vacanti JP. Tissue engineering: The design and fabrication of living replacement devices for surgical reconstruction and transplantation. Lancet 1999;354(supp 1):S132–S134.
15. Zong X, Chung CY, Yin L, Fang D, Hsiao BS, Chu B, Entcheva E. Electrospun fine-textured scaffolds for heart tissue constructs. Biomaterials 2005;26:5330–5338. [PubMed: 15814131]
16. Khil MS, Kim KY, Kim SZ, Lee KH. Novel fabricated matrix via electrospinning for tissue engineering. J Biomed Mater Res B Appl Biomater 2005;15:117–124.
17. Formhals A US Patent 1,975,5042, 1934.
18. Theron SA, Zussman E, Yarin AL. Experimental investigation of the governing parameters in electrospinning of polymer solutions. Polymer 2004;45:217–230.
19. Reneker DH, Kataphinan W, Theron A, Zussman E, Yarin AL. Nanofiber garlands of polycaprolactone by electrospinning. Polymer 2002;43:6785–6794.
20. Bhattarai SR, Yi HK, Hwang PH, Cha DI, Kim HY. Novel biodegradable electrospun membrane: Scaffold for tissue engineering. Biomaterials 2004;25:2595–2602. [PubMed: 14751745]
21. Li WJ, Caterson EJ, Tuan RS, Ko FK. Electrospun nanofibrous structure: A novel scaffold for tissue engineering. J Biomed Mater Res 2002;60:613–621. [PubMed: 11948520]
22. Schenke-Layland K, Nsair A, van Handel B, Angelis E, Gluck JM, Votteler M, Goldhaber JI, Mikkola HKA, Kahn M, MacLellan WR. Recapitulation of the embryonic cardiovascular progenitor cell niche. Biomaterials 2011;32:2748–2756. [PubMed: 21257198]
23. Heydarkhan-Hagvall S, Gluck JM, Delman C, Jung M, Ehsani N, Full S, Shemin RJ. The effect of vitronectin on the differentiation of embryonic stem cells in a 3D culture system. Biomaterials 2012;33:2032–2040. [PubMed: 22169822]
24. Gluck JM, Rahgozar P, Ingle NP, Rofail F, Petrosian A, Cline MG, Jordan MC, Roos KP, MacLellan WR, Shemin RJ, Heydarkhan-Hagvall S. Hybrid co-axial electrospun nanofibrous scaffolds with limited immunological response created for tissue engineering. J Biomed Mater Res Part B 2011;99B:180–190.
25. Cushing MC, Anseth KS. Hydrogel cell cultures. Science 2007;316: 1133–1134. [PubMed: 17525324]
26. L'Heureux N, Dusserre N, Konig G, Victor B, Keire P, Wight TN, Chronos NAF, Kyles AE, Gregory CR, Hoyt G, Robbins RC, McAllister TN. Human tissue-engineered blood vessels for adult arterial revascularization. Nat Med 2006;12:361–365. [PubMed: 16491087]
27. Chiu LL, Radisic M. Scaffolds with covalently immobilized VEGF and angiopoietin-1 for vascularization of engineered tissues. Biomaterials 2010;31:226–241. [PubMed: 19800684]
28. Du F, Wang H, Zhao W, Li D, Kong D, Yang J, Zhang Y. Gradient nanofibrous chitosan/poly-e-caprolactone scaffolds as extracellular microenvironment for vascular tissue engineering. Biomaterials 2012;33:762–770. [PubMed: 22056285]
29. Godier-Furnemont AFG, Martens TP, Koeckert MS, Wan L, Parks J, Arai K, Zhang G, Hudson B, Homma S, Vunjak-Novakovic G. Composite scaffold provides a cell delivery platform for cardiovascular repair. Proc Natl Acad Sci USA 2011;108:7974–7979. [PubMed: 21508321]
30. Aizawa Y, Shoichet MS. The role of endothelial cells in the retinal stem and progenitor cell niche within a 3D engineered hydrogel matrix. Biomaterials 2012;33:5198–5205. [PubMed: 22560669]
31. Wijelath ES, Rahman S, Murray J, Patel Y, Savidge G, Sobel M. Fibronectin promotes VEGF-induced CD34+ cell differentiation into endothelial cells. J Vasc Surg 2004;39:655–660. [PubMed: 14981463]
32. Wijelath ES, Murray J, Rahman S, Patel Y, Ishida A, Stand K, Aziz S, Cardona C, Hammond WP, Savidge GF, Rafii S, Sobel M. Novel vascular endothelial growth factor binding domains of fibronectin enhance vascular endothelial growth factor biological activity. Circ Res 2002;91:25–31. [PubMed: 12114318]
33. Risau W, Flamme I. Vasculogenesis. Annu Rev Cell Dev Biol 1995; 11:73–91. [PubMed: 8689573]
34. Krawiec JT, Vorp DA. Adult stem cell-based tissue engineered blood vessels: A review. Biomaterials 2012;33:3388–3400. [PubMed: 22306022]

35. De Visscher G, Mesure L, Meuris B, Ivanova A, Flameng W. Improved endothelialization and reduced thrombosis by coating a synthetic vascular graft with fibronectin and stem cell homing factor SDF-1α. Acta Biomater 2012;8:1330–1338. [PubMed: 21964214]

36. Pimton P, Sarker S, Sheth N, Perets A, Marcinkiewicz C, Lazarovici P, Lelkes P. Fibronectin-mediated upregulation of a5b1 integrin and cell adhesion during differentiation of mouse embryonic stem cells. Cell Adh Migr 2011;5:73–82. [PubMed: 20962574]

37. Ferreira LS, Gerecht S, Fuller J, Shieh HF, Vunjak-Novakovic G, Langer R. Bioactive hydrogel scaffolds for controllable vascular differentiation of human embryonic stem cells. Biomaterials 2007; 28:2706–2717. [PubMed: 17346788]

38. Davies MG, Hagen PO. Pathophysiology of vein graft failure: A review. Eur J Vasc Endovasc Surg 1995;9:7–18. [PubMed: 7664016]

39. Rotmans JI, Heyligers JMM, Stroes ESG, Pasterkamp G. Endothelial progenitor cell-seeded grafts: Rash and risky. Can J Cardiol 2006;22:1113–1116. [PubMed: 17102827]

40. Welch M, Durrans D, Carr HM, Vohra R, Rooney OB, Walker MG. Endothelial cell seeding: A review. Ann Vasc Surg 1992;6:473–484. [PubMed: 1467191]

41. Davie EW. Biochemical and molecular aspects of the coagulation cascade. Thromb Haemostasis 1995;74:1–6. [PubMed: 8578439]

42. Mun CH, Jung Y, Kim SH, Lee SH, Kim HC, Kwon IK, Kim SH. Three-dimensional electrospun poly(lactide-co-e-caprolactone) for small-diameter vascular grafts. Tissue Eng Part A 2012;18:1608–1616. [PubMed: 22462723]

43. Zhao J, Liu L, Wei J, Ma D, Gen W, Yan X, Zhu J, Du H, Liu Y, Li L, Chen F. A novel strategy to engineer small-diameter vascular grafts from marrow-derived mesenchymal stem cells. Artif Organs 2012;36:93–101. [PubMed: 21790675]

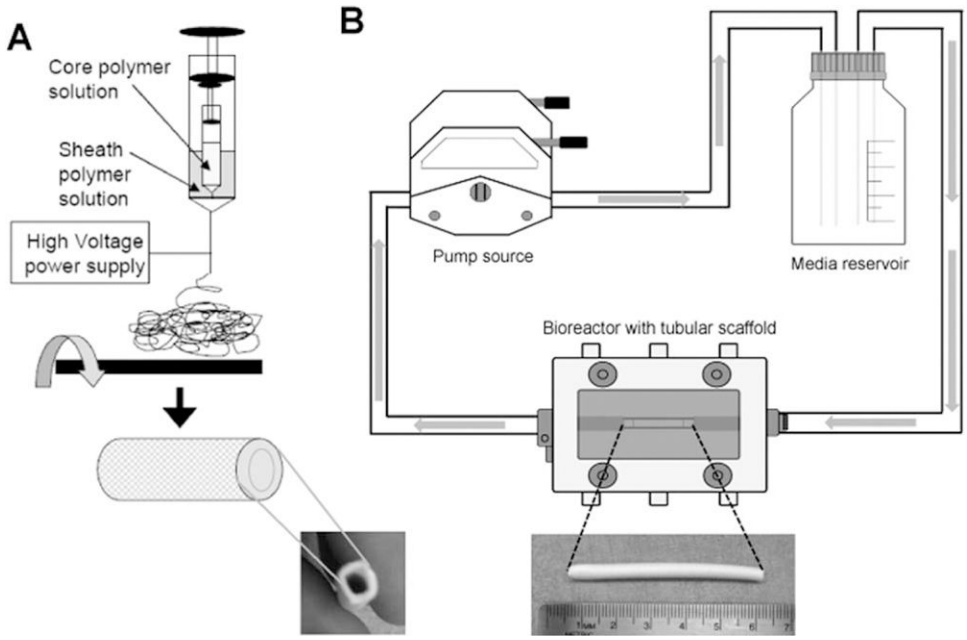

FIGURE 1.

Electrospun tubular scaffold fabrication. Electrospun fibers were collected on a rotating mandrel (A). The electrospun tubular scaffolds were placed in a bioreactor chamber and seeded with Flk-1^{+} CPCs. Media from the reservoir was pumped through the lumen of the tubular scaffold at a controlled and sustained pressure of 120 mmHg.

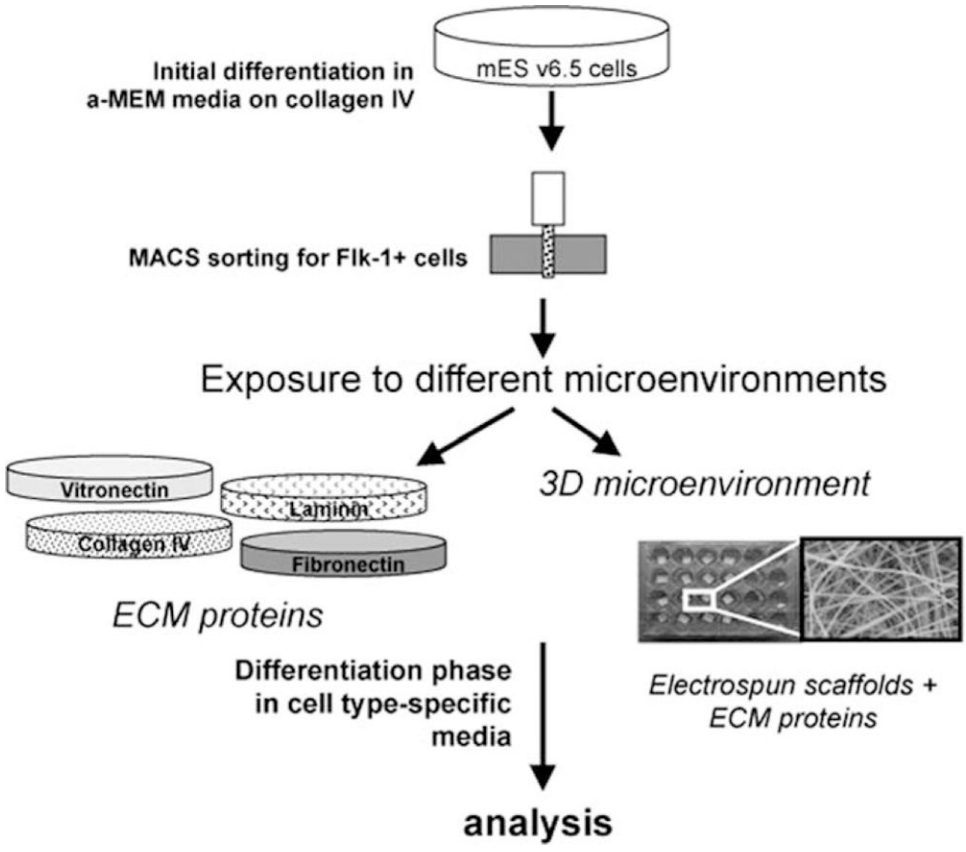

FIGURE 2.

Experimental Design. Schematic depicting experimental design. mES cells were expanded in initial differentiation media and then sorted for Flk-1^{+} CPCs. Isolated CPCs were then exposed to various microenvironments in both 2D and 3D and analyzed at day 7 or 14.

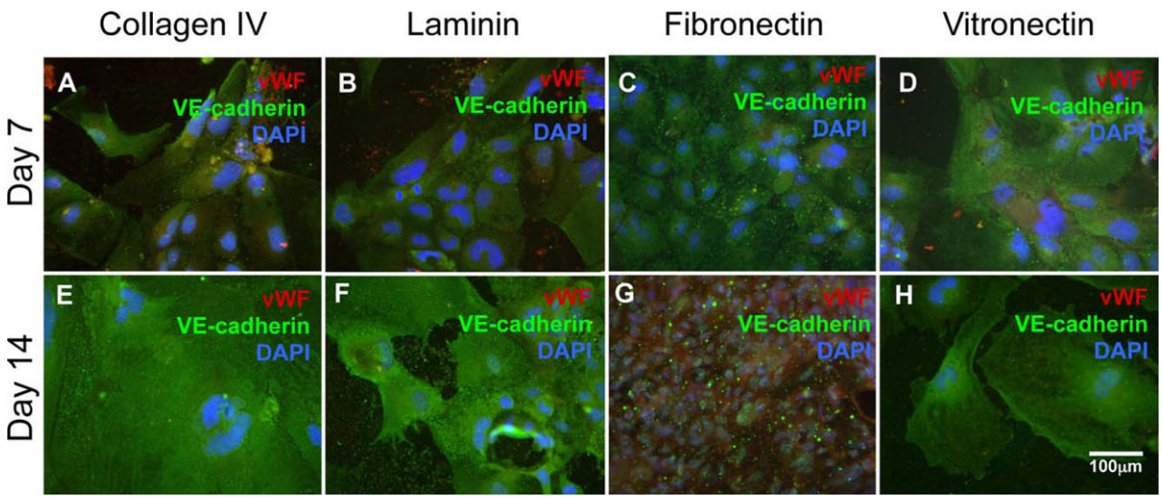

FIGURE 3.

Vascular endothelial cell differentiation. mES cell-derived Flk-1^{+} CPCs were exposed to different microenvironments for both 7 and 14 days. Cells were analyzed for vWF (red) and VE-cadherin (green).

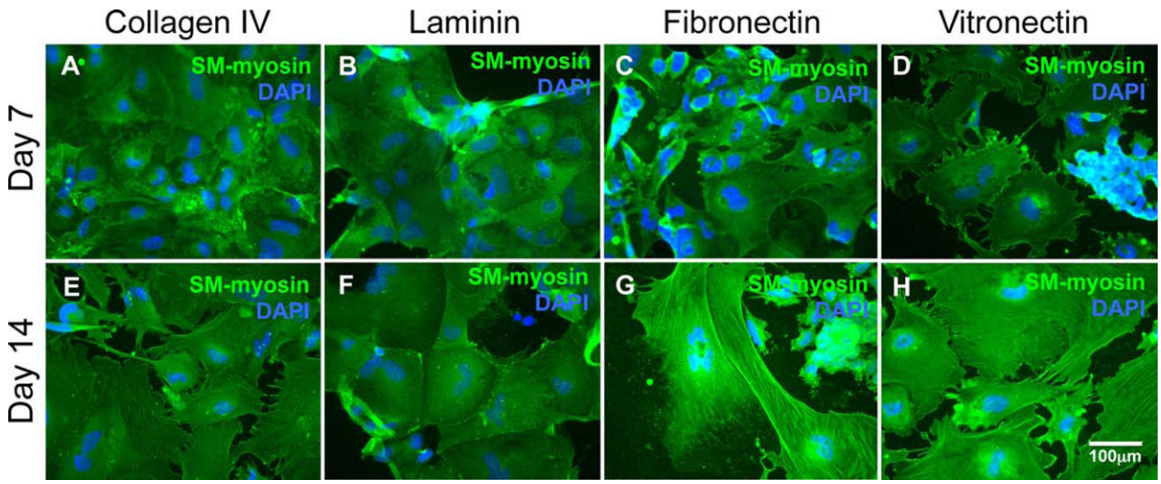

FIGURE 4.

Vascular smooth muscle cell differentiation. mES cell-derived Flk-1^{+} CPCs were exposed to different microenvironments for both 7 and 14 days. Cells were analyzed for SM-myosin (green).

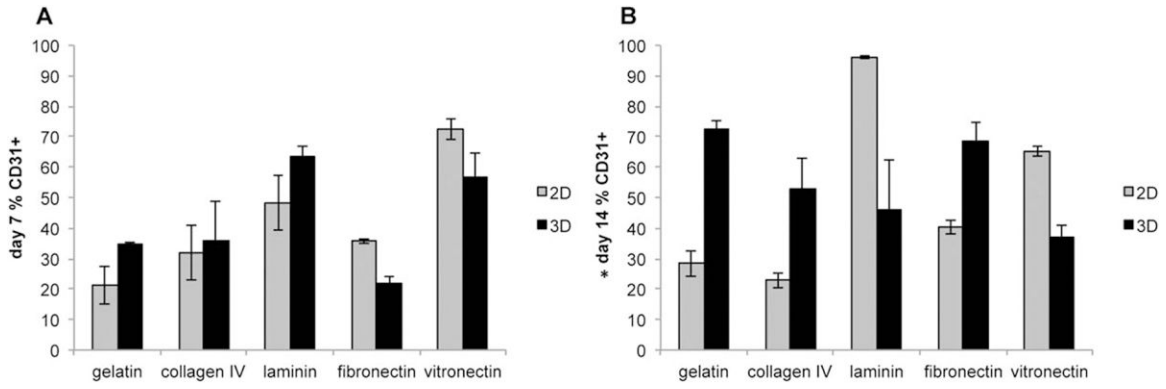

FIGURE 5.

FACS analysis of vascular endothelial cells. Flk-1^+ CPCs were exposed to different microenvironments in both 2D (grey bars) and 3D (black bars) for both 7 (A) and 14 (B) days. CD31 was used as a cell surface marker for endothelial cells for FACS analysis. There was a significant difference increase in CD31 expression on day 14 compared to day 7. $N = 3$ *$p < 0.05$ for pairwise statistical comparison.

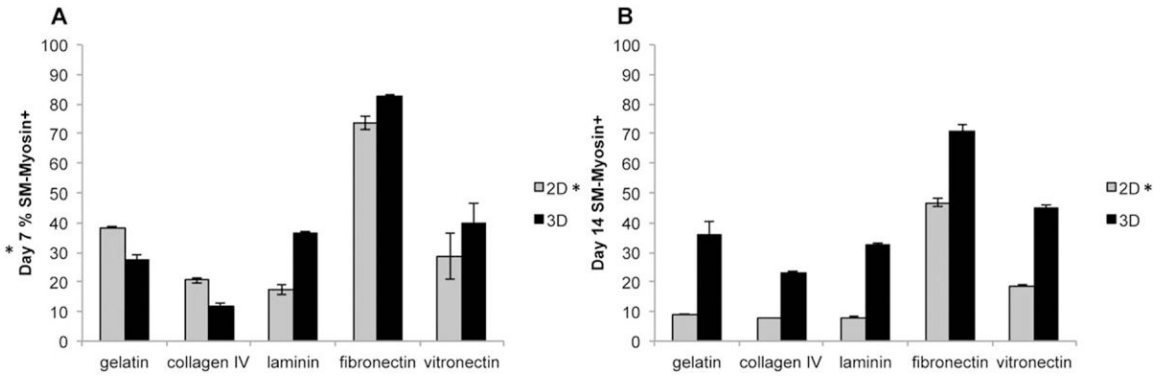

FIGURE 6.

FACS analysis of vascular smooth muscle cells. Flk-1^{+} CPCs were exposed to different microenvironments in both 2D (grey bars) and 3D (black bars) for both 7 (A) and 14 (B) days. SM-myosin was used as a marker for FACS analysis. There was a significantly higher expression of myosin for day 7 compared to day 14. Likewise, at each time point there was a significant difference between 2D and 3D culture system. $N = 3$ *$p < 0.0001$ for pairwise statistical comparison.

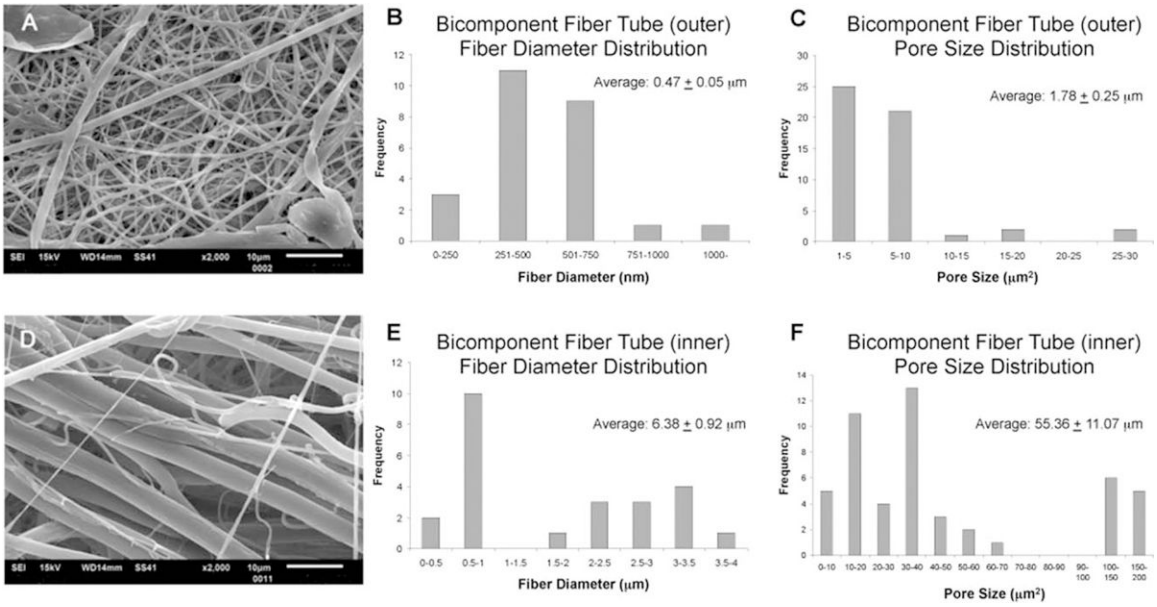

FIGURE 7.

Physical properties of electrospun tubular scaffold. Representative SEM micrographs show the fiber morphology of the outer most layer of fibers (A) and inner most layer (D). Fiber diameter distributions were calculated for the outer most layer fibers (B) and the inner most layer (E). Pore size distributions were also calculated for the outer fibers (C) and inner fibers (F).

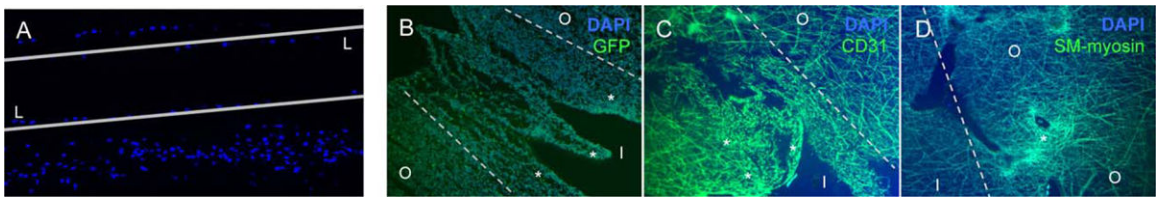

FIGURE 8.

Immunofluorescent imaging of the electrospun tubular scaffold after 30 days in the bioreactor chamber. Cells were found evenly distributed throughout the cross-section of the tubular scaffold. The lumen of the scaffold is denoted by "L" and the lines represent the boundaries of the scaffold (A). The existence of CPC-derived cell layers is found by the higher concentration of green fluorescence—more GFP^+ cells (shown with *) which were seeded second are found in the inner most circumference (denoted as "I") of the tubular scaffold (B); more $CD31^+$ cells (shown with *) which were seeded second are found in the inner most circumference or lumen (C); more SM-$myosin^+$ cells (shown with *) which were seeded first are found on the outer most circumference of the tubular scaffold (denoted as "O") (D).